NUMERICAL MODELING OF NON-ISOTHERMAL FILTRATION OF NATURAL GAS

V. I. VASIL'EV (iD)
A. V. AMMOSOV (iD)

COMMUNICATED BY M. A. SHISHLENIN

Abstract: In the article of numerical modeling of non-isothermal filtration of natural gas through a single well in axisymmetric coordinates is carried out using the finite difference method. The mathematical model of natural gas uses the Latonov-Gurevich supercompressibility coefficient. Discretization of the mathematical model is carried out using linearized and implicit difference schemes on a quasi-uniform space-time grid. Results of numerical simulation are presented.

Keywords: filtration equation, supercompressibility coefficient, adiabatic expansion, Joule-Thomson effect, finite difference method, splitting method.

1 Introduction

The Arctic and North-Eastern regions of the country have huge reserves of hydrocarbon raw materials. To develop them, it is necessary to incur additional

costs for solving infrastructural problems of field development, developing environmentally safety technologies for the extraction of hydrocarbons and their transportation. In addition, global climate change introduces additional difficulties in the construction and operation of oil and gas production facilities.

Taking into account the processes occurring during the development of gas, oil and gas, and gas condensate fields is of great importance for balanced control and maintenance of the temperature regime around operating wells [1-7]. Gas production technologies can be quite different depending on the location of the fields, possible water content, heterogeneity and fracturing in the formations, and containing permafrost soils [8,13-15,20]

These processes are described using numerous mathematical models based on the fundamental laws of continuum mechanics [4-12]. The mathematical model of natural gas extraction from a reservoir is described by an interconnected nonlinear system of partial differential equations. It is based on the fundamental laws of conservation of mass and energy, Darcy's law, the equation of state of a real gas with a gas supercompressibility coefficient determined by the empirical Latonov-Gurevich formula [16]. It should be noted that the law of conservation of energy describes several physical processes: conductive and convective heat transfer, the Joule-Thomson effect and adiabatic expansion inherent in natural gas [14, 16]. In [20], it is shown that the Redlich-Kwong equation, widely used for calculating the behavior of mixtures of natural gases, allows one to thermodynamically adequately construct an inversion curve corresponding to a change in the sign of the Joule-Thomson coefficient. In [19] considers numerical modeling of water flow in porous media under conditions close to critical.

Numerical methods modeling of fluid flow in cracks with explisit scheme and implicit scheme by the finite difference method are presented in [10,11,17]. Numerical modeling can describe detailed changes in parameters (coefficient of thermal conductivity, coefficient of heat capacity, temperature, etc.), which are difficult to measure experimentally, at all time intervals. The difficulties encountered in solving by the finite difference method are most effectively overcome by the method of splitting by physical processes [13, 14].

In this paper, we consider and compare two differential schemes constructed by the finite difference method: a linearized implicit difference scheme and an implicit difference scheme implemented by iterations over non-linear ones. The purpose of this work is a numerical comparison of the calculation results for both difference schemes. At the same time, when constructing an implicit difference scheme, the method of splitting by physical processes was used.

The paper consists of seven Sections. In the first Section, we provide an overview of research on the subject of the article. In the second Section, we devoted ourselves to the selection of a mathematical model for the development of a natural gas field. In the third Section, a linearized difference scheme is constructed in which the nonlinear coefficients of the discrete analog are taken from the lower time layer. The purely implicit finite difference analogue of a nonlinear initial boundary value problem for a system of parabolic equations is constructed in the fourth Section. Its iterative implementation is described in Section 5. The results of the computational experiment are presented in the sixth Section. The seventh Section contains the conclusions.

2 Mathematical model of non-isothermal filtration of natural gas

We describe numerical study of an axisymmetric non-isothermic inflow of natural gas to a well of radius r_c in the area $\Omega = (r_c, R_k)$, where R_k is the radius of the reservoir contour. Continuity equation of of the gas flow [15]:

$$m\frac{\partial}{\partial t}\Big(\frac{p}{Tz}\Big) = \frac{1}{r}\frac{\partial}{\partial r}\Big(\frac{k}{\mu_g}\frac{p}{Tz}r\frac{\partial p}{\partial r}\Big), \quad r \in \Omega, \quad t \in (0,\bar t], \tag{1}$$

where k is the permeability coefficient of a porous medium, μ_g is the dynamic viscosity of the natural gas, m is the porosity, r is the radius, p is the pressure and T is the temperature of the natural gas.

The calculation results of the Latonov–Gurevich equation of gas supercompressibility coefficient in [17] showed a good correspondence. Therefore, the gas supercompressibility coefficient z we will calculate by using the Latonov–Gurevich equation [16]:

$$z(p,T) = \Big[0.17376ln\Big(\frac{T}{T_c}\Big) + 0.73\Big]^{\frac{p}{p_c}} + 0.1\frac{p}{p_c}, \tag{2}$$

where $T_c = 190.5$ K and $p_c = 45.8\cdot10^5$ Pa are the critical values of gas temperature and pressure.
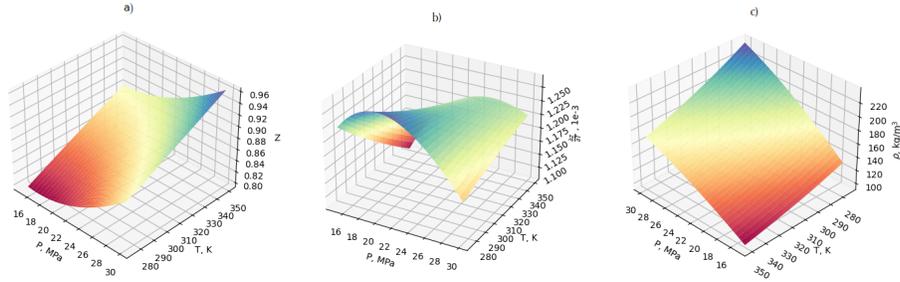

Figure 1. a) A graph of the coefficient of supercompressibility; b) a graph of the partial derivative of the coefficient of supercompressibility; c) density

This Figure 1 defines and shows the changes in a) the values of the supercompressibility coefficient, b) the partial derivative of the supercompressibility coefficient, and c) density under appropriate temperature conditions and pressure in the collector. According to graph a), the coefficient of supercompressibility z varies from 0.8 to 0.96 for an operating well in which the pressure and temperature decrease, which means a decrease in the coefficient of supercompressibility. For the partial derivative of the supercompressibility coefficient $\frac{\partial z}{\partial T}$, the changes will be significant: it varies from $1\cdot10^{-3}$ to $1.25\cdot10^{-3}$. The density of ρ varies from 100 kg/m^3 to 220 kg/m^3, in the vicinity of an operating well with a decrease in pressure and temperature.

The law of conservation of energy is described by the equation [15]:

$$C\rho\frac{\partial T}{\partial t} = \frac{1}{r}\frac{\partial}{\partial r}\Big(r\lambda\frac{\partial T}{\partial r}\Big) + m\Big(1 + \frac{T}{z}\frac{\partial z}{\partial T}\Big)\frac{\partial p}{\partial t} + C_p\frac{k}{\mu_g}\frac{p}{RTz}\frac{\partial p}{\partial r}\frac{\partial T}{\partial r} \tag{3}$$

$$-\frac{k}{\mu_g}\frac{T}{z}\frac{\partial z}{\partial T}\Big(\frac{\partial p}{\partial r}\Big)^2, \quad r \in \Omega, \quad t \in (0,\bar t].$$

Initial conditions:

$$p(r,0) = p_0, \quad r \in \overline{\Omega}, \quad t = 0, \tag{4}$$

$$T(r,0) = T_0, \quad r \in \overline{\Omega}, \quad t = 0. \tag{5}$$

At the well bottom, the mass influx of gas is set:

$$2\pi r_c \frac{k}{\mu_g} H \frac{p}{RTz} \frac{\partial p}{\partial r} = M, \quad r = r_c, \quad t \in (0, \overline{t}] \tag{6}$$

boundary conditions:

$$\frac{\partial p}{\partial r} = 0, \quad r = R_k, \quad t \in (0, \overline{t}], \tag{7}$$

$$\frac{\partial T}{\partial r} = 0, \quad r = R_k, \quad t \in (0, \overline{t}]. \tag{8}$$

3 Linearized implicit difference scheme

The numerical solution of a nonlinear system of partial differential equations with corresponding boundary and initial conditions (1) – (8) will be carried out using the finite-difference method. For this purpose, in the solution domain Ω we will introduce a quasi-uniform space-time grid $\omega_{h\tau}$:

$$\overline{\omega}_{h\tau} = \overline{\omega}_h \times \overline{\omega}_\tau,$$

where

$$\overline{\omega}_h = \{h_i = q_1 h_{i-1}, \quad i = 1, 2, \ldots, n\},$$

$$\overline{\omega}_\tau = \{\tau^j = q_2 \tau^{j-1}, \quad j = 1, 2, \ldots, m\}$$

In this difference scheme, all nonlinear coefficients of the difference equations are taken from the lower time layer:

$$\begin{aligned}
\frac{m r_i \hbar_i}{\tau \check{T}_i \check{z}_i} \left(p_i - \check{p}_i \right) &= \left(r \frac{k}{\mu} \frac{\check{p}}{\check{T}\check{z}} \right)_{i+0.5} \frac{p_{i+1} - p_i}{h_{i+1}} \\
&- \left(r \frac{k}{\mu} \frac{\check{p}}{\check{T}\check{z}} \right)_{i-0.5} \frac{p_i - p_{i-1}}{h_i}, \qquad i = 1, 2\ldots, n-1.
\end{aligned} \tag{9}$$

Discretization of the boundary condition (6) at the well bottom

$$\frac{m r_0 \hbar_0}{\tau \check{T}_0 \check{z}_0} \left(p_0 - \check{p}_0 \right) = \left(r \frac{k}{\mu} \frac{\check{p}}{\check{T}\check{z}} \right)_{0.5} \frac{p_1 - p_0}{h_1} - \frac{MR}{2\pi H}. \tag{10}$$

We supplement the system of equations (9), (10) with a discrete analogue of the boundary condition (7) and the initial condition (4)

$$\frac{m r_n \hbar_n}{\tau \check{T}_n \check{z}_n} \left(p_n - \check{p}_n \right) = -\left(r \frac{k}{\mu} \frac{\check{p}}{\check{T}\check{z}} \right)_{n-0.5} \frac{p_n - p_{n-1}}{h_n}. \tag{11}$$

$$p(r,0) = p_0(r), \quad r \in \omega_h. \tag{12}$$

To determine the discrete analogue of temperature on the auxiliary layer of the splitting method by physical processes, we construct a linearized difference scheme:

$$
C\rho_i \frac{\overline{T}_i - \check{T}_i}{\tau} = m\left(1 + \left(\frac{\check{T}}{\check{z}}\frac{\partial\check{z}}{\partial\check{T}}\right)_i\right)\frac{p_i - \check{p}_i}{\tau} + C_p\left(\frac{kp}{\mu R\check{z}\check{T}}\right)_i \frac{p_{i+1} - p_i}{h_{i+1}}
$$
$$
\frac{\overline{T}_{i+1} - \overline{T}_i}{h_{i+1}} - \left(\frac{k}{\mu}\frac{\check{T}}{\check{z}}\frac{\partial\check{z}}{\partial\check{T}}\right)_i \left(\frac{p_{i+1} - p_i}{h_{i+1}}\right)^2, \qquad i = n-1, n-2, \ldots, 0. \tag{13}
$$

Since the parameters of equation (9) comes from the boundary $r_n = R_k$, we supplement the system of equations (10) with a discrete analogue of the initial condition (5):

$$
\overline{T}_n = T_0. \tag{14}
$$

we use a purely implicit scheme for equation (10) :

$$
C\rho_i r_i \hbar_i \frac{T_i - \overline{T}_i}{\tau} = (r\lambda)_{i+1/2}\frac{T_{i+1} - T_i}{h_{i+1}} -
$$
$$
(r\lambda)_{i-1/2}\frac{T_i - T_{i-1}}{h_i}, \quad i = 1, 2, \ldots, n-1. \tag{15}
$$

Discrete analogues of boundary conditions and conjugation conditions:

$$
T_0 = \overline{T}_0, \tag{16}
$$
$$
T_n = \overline{T}_n, \tag{17}
$$
$$
T(r,t) = \overline{T}(r,t), \tag{18}
$$

and initial conditions:

$$
T(r,0) = T_0(r). \tag{19}
$$

4   Implicit difference scheme

We construct a discrete analogue in space of the boundary value problem under consideration, to solve the equation (1) by the finite difference method. For this, we use a purely implicit scheme:

$$
\frac{mr_i\hbar_i}{\tau}\left(\frac{p_i}{T_i z_i} - \frac{\check{p}_i}{\check{T}_i \check{z}_i}\right) = \left(r\frac{k}{\mu}\frac{p}{Tz}\right)_{i+0.5}\frac{p_{i+1} - p_i}{h_{i+1}}
$$
$$
-\left(r\frac{k}{\mu}\frac{p}{Tz}\right)_{i-0.5}\frac{p_i - p_{i-1}}{h_i}, \qquad i = 1, 2 \ldots, n-1. \tag{20}
$$

Discretization of the boundary condition (6) at the well bottom

$$
\frac{mr_0\hbar_0}{\tau}\left(\frac{p_0}{T_0 z_0} - \frac{\check{p}_0}{\check{T}_0 \check{z}_0}\right) = \left(r\frac{k}{\mu}\frac{p}{Tz}\right)_{0.5}\frac{p_1 - p_0}{h_1} - \frac{MR}{2\pi H}. \tag{21}
$$

We supplement the system of equations (20), (21) with a discrete analogue of the boundary condition (7) and the initial condition (4):

$$
\frac{mr_n\hbar_n}{\tau}\left(\frac{p_n}{T_n z_n} - \frac{\check{p}_n}{\check{T}_n \check{z}_n}\right) = -\left(r\frac{k}{\mu}\frac{p}{Tz}\right)_{n-0.5}\frac{p_n - p_{n-1}}{h_n}. \tag{22}
$$
$$
p(r,0) = p_0(r), \quad r \in \omega_h. \tag{23}
$$

The non-stationary quasilinear partial differential equation (1) simultaneously describes several physical processes: conductive and convective heat transfer, the throttling effect during gas flow, and the adiabatic expansion of a moving gas. The difficulties encountered in solving this equation are effectively overcome by splitting

into physical processes [15, 16]. This method uses a transition from the $(j-1)$-th time layer to the j-th in two stages:

$$C_n \frac{\partial \overline{T}}{\partial t} = m\Big(1 + \frac{\overline{T}}{z}\frac{\partial z}{\partial T}\Big)\frac{\partial p}{\partial t} + C_p \frac{k}{\mu_g}\frac{p}{R\overline{T}z}\frac{\partial p}{\partial r}\frac{\partial \overline{T}}{\partial r} - \frac{k}{\mu_g}\frac{\overline{T}}{z}\frac{\partial z}{\partial T}\Big(\frac{\partial p}{\partial r}\Big)^2, \tag{24}$$

$$r \in [r_c, R_k), \quad t \in (t_{j-1}, t_j],$$

$$C_n \frac{\partial T}{\partial t} = \frac{1}{r}\frac{\partial}{\partial r}\Big(r\lambda_n \frac{\partial T}{\partial r}\Big), \quad r \in (r_c, R_k), \quad t \in (t_{j-1}, t_j]. \tag{25}$$

with the conjugation conditions:

$$\overline{T}(r, t_{j-1} = T(r, t_{j-1}), \quad r \in [r_c, R_k] \tag{26}$$

$$T(r, t_{j-1}) = \overline{T}(r, t_j), \quad r \in [r_c, R_k] \tag{27}$$

$$T(r_c, t_{j-1}) = \overline{T}(r_c, t_j), \quad t \in (t_{j-1}, t_j] \tag{28}$$

Equation (20) is a first-order hyperbolic equation. The solution of this equation is carried out from the right boundary, so the boundary condition (8) is sufficient to find the only solution.

The choice of the boundary condition (8) is explained by the fact that near the well, the convective term of the equation (1) significantly exceeds the conductive component.

We use a stable implicit difference scheme for the function $T(r, t)$:

$$C\rho_i \frac{\overline{T}_i - \check{T}_i}{\tau} = m\left(1 + \Big(\frac{\overline{T}}{z}\frac{\partial z}{\partial T}\Big)_i\right)\frac{p_i - \check{p}_i}{\tau} + C_p\Big(\frac{kp}{\mu R\overline{T}z}\Big)_i \frac{p_{i+1} - p_i}{h_{i+1}}$$
$$\frac{\overline{T}_{i+1} - \overline{T}_i}{h_{i+1}} - \Big(\frac{k}{\mu}\frac{\overline{T}}{z}\frac{\partial z}{\partial T}\Big)_i\Big(\frac{p_{i+1} - p_i}{h_{i+1}}\Big)^2, \qquad i = n-1, n-2, \ldots, 0. \tag{29}$$

Since the parameters of equation (20) comes from the boundary $r_n = R_k$, we supplement the system of equations (21) with a discrete analogue of the initial condition (5):

$$\overline{T}_n = T_0. \tag{30}$$

we use a purely implicit scheme for equation (21) :

$$C\rho_i r_i \hbar_i \frac{T_i - \overline{T}_i}{\tau} = (r\lambda)_{i+1/2}\frac{T_{i+1} - T_i}{h_{i+1}} -$$
$$(r\lambda)_{i-1/2}\frac{T_i - T_{i-1}}{h_i}, \quad i = 1, 2, \ldots, n-1. \tag{31}$$

Discrete analogues of boundary conditions and conjugation conditions:

$$T_0 = \overline{T}_0, \tag{32}$$

$$T_n = \overline{T}_n, \tag{33}$$

$$T(r, t) = \overline{T}(r, t), \tag{34}$$

and initial conditions:

$$T(r, 0) = T_0(r). \tag{35}$$

5   Iterative implementation of the difference scheme

We construct a discrete analogue in space of the boundary value problem under consideration to solve the equation (2) by the finite difference method. For this, we use a purely implicit scheme:

$$
\begin{aligned}
\frac{mr_i\hbar_i}{\tau}\Big(\frac{p_i^{s+1}}{T_i^s z_i^s} - \frac{\check{p}_i}{\check{T}_i\check{z}_i}\Big) &= \Big(\frac{rkp^s}{\mu T^s z^s}\Big)_{i+0.5}\frac{p_{i+1}^{s+1} - p_i^{s+1}}{h_{i+1}} \\
&- \Big(\frac{rkp^s}{\mu T^s z^s}\Big)_{i-0.5}\frac{p_i^{s+1} - p_{i-1}^{s+1}}{h_i}, \qquad i = 1, 2\ldots, n-1.
\end{aligned}
\tag{36}
$$

Discrete analogue of the boundary condition (6) at the well bottom

$$
\frac{mr_0\hbar_0}{\tau}\Big(\frac{p_0^{s+1}}{T_0^s z_0^s} - \frac{\check{p}_0}{\check{T}_0\check{z}_0}\Big) = \Big(\frac{rkp^s}{\mu T^s z^s}\Big)_{0.5}\frac{p_1^{s+1} - p_0^{s+1}}{h_1} - \frac{MR}{2\pi H}.
\tag{37}
$$

We supplement the system of equations (36), (37) with a discrete analogue of the boundary condition (7) and the initial condition (4):

$$
\frac{mr_n\hbar_n}{\tau}\Big(\frac{p_n^{s+1}}{T_n^s z_n^s} - \frac{\check{p}_n}{\check{T}_n\check{z}_n}\Big) = -\Big(\frac{rkp^s}{\mu T^s z^s}\Big)_{n-0.5}\frac{p_n^{s+1} - p_{n-1}^{s+1}}{h_n}.
\tag{38}
$$

For the function $T(r,t)$ we use a stable implicit difference scheme:

$$
\begin{aligned}
C\rho_i^s\frac{\overline{T}_i^{s+1} - \check{T}_i}{\tau} &= m\Bigg(1 + \Big(\frac{\overline{T}}{z}\frac{\partial z}{\partial T}\Big)_i^s\Bigg)\frac{p_i^{s+1} - \check{p}_i}{\tau} + C_p\Big(\frac{k}{R\mu}\frac{p}{\overline{T}z}\Big)_i\frac{p_{i+1}^{s+1} - p_i^{s+1}}{h_{i+1}} \\
&\frac{\overline{T}_{i+1} - \overline{T}_i}{h_{i+1}} - \Big(\frac{k}{\mu}\frac{\overline{T}}{z}\frac{\partial z}{\partial T}\Big)_i\Big(\frac{p_{i+1}^{s+1} - p_i^{s+1}}{h_{i+1}}\Big)^2, \; i = n-1, n-2, \ldots, 0.
\end{aligned}
\tag{39}
$$

we use next notations:

$$
z_i = z(p_i^{s+1}, T_i^s), \quad \Big(\frac{\partial z}{\partial T}\Big)_i = \Big(\frac{\partial z(p_i^{s+1}, T_i^s)}{\partial T_i^s}\Big), \quad \Big(\frac{p}{\overline{T}z}\Big)_i = \frac{p_i^{s+1}}{\overline{T}_i^s z(p_i^{s+1}, \overline{T}_i^s)}.
$$

Since the parameters in the equation (36) comes from the boundary $r_n = R_k$, we supplement the system of equations (37) by a discrete analog of the initial condition (5):

$$
\overline{T}_n = T_0, \quad t \in \omega_{h\tau}.
\tag{40}
$$

For the equation (37), we use a purely implicit scheme:

$$
\begin{aligned}
C_i r_i\hbar_i\frac{T_i - \overline{T}_i}{\tau} &= (r\lambda)_{i+1/2}\frac{T_{i+1} - T_i}{h_{i+1}} - \\
(r\lambda)_{i-1/2}&\frac{T_i - T_{i-1}}{h_i}, \quad i = 1, 2, \ldots, n-1.
\end{aligned}
\tag{41}
$$

Discrete analogs of boundary conditions and conjugation conditions:

$$
T_0^{s+1} = \overline{T}_0,
\tag{42}
$$

$$
T_n^{s+1} = \overline{T}_n,
\tag{43}
$$

$$
T_i^0 = \overline{T}_i^{s+1}(r, t).
\tag{44}
$$

6 Numerical results

We present of numerical results of one-dimensional problem of natural gas filtration with input data taken from [14] in the international SI system:

$m = 0.2$ – porosity;

$r_c = 0.08m$ – radius of well;

$R_k = 4000m$ – radius of the collector contour;

$H = 27m$, $10m$, $3m$ – reservoir thickness (3 options);

$R = 520\text{J}/(\text{kg·K})$ – Gas constant;

$\mu = 2 \cdot 10^{-5}$ Pa· s – dynamic viscosity of the natural gas;

$C_p = 2000 \cdot \text{J}/(\text{kg·K})$ – Specific heat capacity

$C\rho = 2.7 \cdot 10^6 \text{J}/(\text{kg·K})$ – Volumetric heat capacity;

$\lambda_n = 1.163\text{W}/(\text{m·K})$ – thermal conductivity coefficient;

$T_0 = 332K$ – initial temperature of the collector;

$p_0 = 2.7 \cdot 10^7$ Pa – initial pressure of the collector;

$M = 4$ kg/s – gas mass flow;

$k = 10^{-13}$ m^2, $5 \cdot 10^{-14}$ m^2, 10^{-14} m^2 – permeability coefficient;

$q_1 = 1.005$, $q_2 = 1.064$ – denominators of the geometric progression of quasi-uniform grids in terms of spatial variable and time.
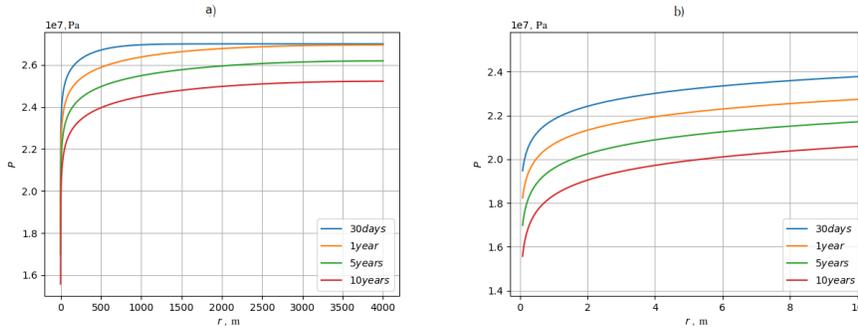

Figure 2. Pressure distribution of natural gas in the reservoir at different time points at $k = 10^{-14}\text{m}^2$ and $H = 10$m a) graph over the entire gas-bearing reservoir; b) graph in the well bottom zone up to 10 m

The calculations were carried out using a linearized implicit difference scheme.

In Fig. 2 and 3, the pressure and temperature distributions along the radius of natural gas in the reservoir after 30 days, 1 year, 5 years, and 10 years from the start of the gas production well at a reservoir thickness of H = 10 m and permeability coefficient k = 10^{-14} m^2. From Fig. 2, in the estimated time of 10 years, the pressures in the bottomhole zone and on the reservoir contour become $1.58 \cdot 10^7$ Pa and $2.53 \cdot 10^7$ Pa, respectively, while a sharp decline is observed at the bottom of the well.

In Fig. 3, at the estimated time of 10 years, there is a temperature change in the well bottom zone within a radius of r = 417 m with a minimum temperature value at the bottom of T = 329.1K, while over time the temperature changes more along the radius than in depth.
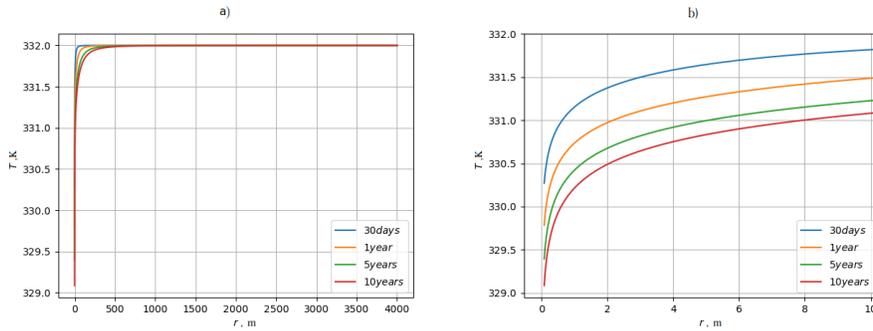
Figure 3. Temperature distribution at different time points with $k = 10^{-14} \text{m}^2$ and $H = 10\text{m}$ a) graph over the entire gas-bearing reservoir; b) graph in the well bottom zone up to 10 m
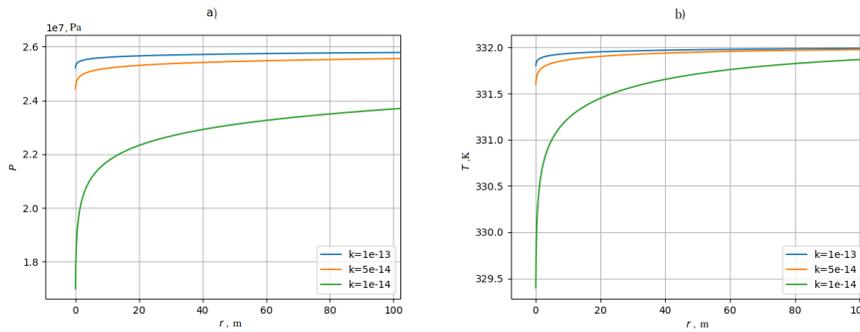

Figure 4. Distribution a) of pressure b) of temperature of natural gas in the reservoir at different values of permeability coefficient for H = 10 m after 5 years of the start of the production well in the well bottom zone up to 100 m
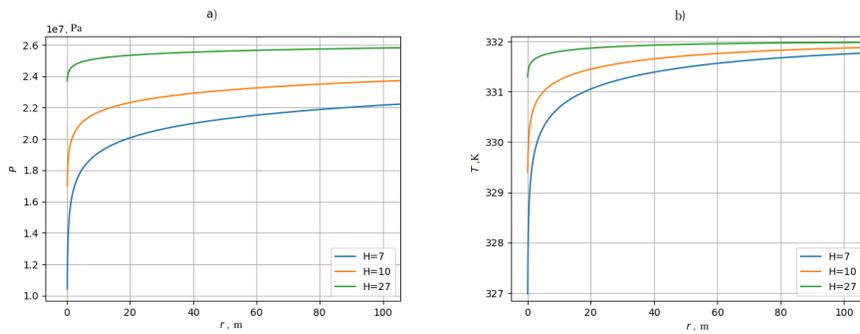

Figure 5. Distribution a) of pressure, b) of temperature of natural gas in reservoir for different values of reservoir thicknesses for k = 10^{-14} m² after 5 years of the start of the production well in the well bottom zone up to 100 m

Figure 4 shows the results of a computational experiment conducted using a linearized implicit scheme for different values of permeability coefficients k = 10^{-13} m², $5 \cdot 10^{-14}$ m², and 10^{-14} m², with a reservoir thickness $H = 10$ meters. It can

be seen from the above graphs that with a permeability coefficient $k = 10^{-14}$ and with constant values of mass flow M and reservoir thickness H, the surface pressure and temperatures decrease more than with a greater permeability coefficient $k = 10^{-13}$ m^2.

Figure 5 shows the results of numerical calculations for different reservoir thicknesses, H = 7 m, 10 m, and 27 m, with permeability coefficient $k = 10^{-14}$ m^2 for a time interval of 5 years from the start of the production well. With a reservoir thickness H = 7 m, the temperature and pressure of natural gas in the target zone fall faster than at the same time with a higher reservoir thickness H = 27 m.
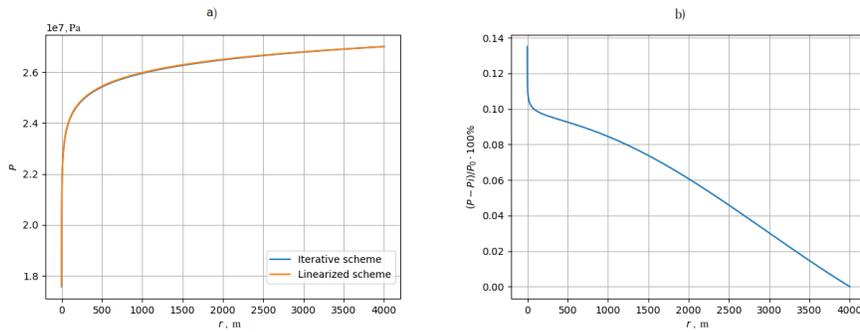

Figure 6. a) A graph of the pressure distribution in the reservoir for the linearized and iterative implementation of the implicit difference scheme 5 years after the start of the production well, b) a graph of the relative deviation between the pressures calculated by both schemes
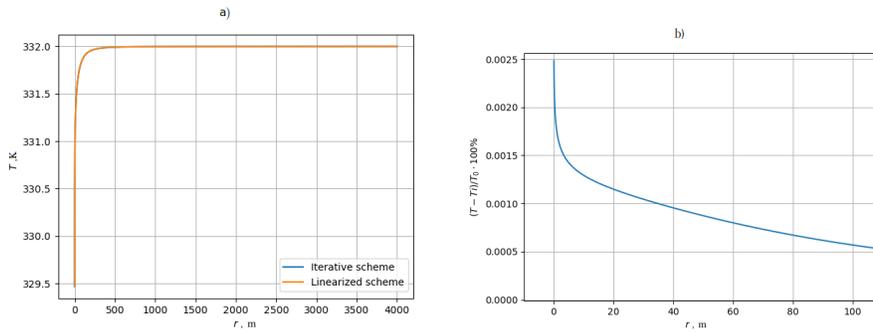

Figure 7. a) A graph of the temperature distribution in the reservoir for the linearized and iterative implementation of the implicit difference scheme after 5 years of starting the production well, b) a graph of the relative deviation between the temperatures calculated by both schemes

According to these figures 6 and 7, it can be concluded that the relative discrepancy between the solutions of the problem obtained using the linearized difference scheme and the iterative implementation of the implicit difference scheme 5 years after the start of the production well launch is less than 0.14% for pressure $(p - pi)/p_0 \cdot 100\%$ in the bottomhole zone and decreases when approaching the collector end, and also

less than 0.0025% for temperature $(T - Ti)/T_0 \cdot 100\%$ in the bottomhole zone and decreases at $i \to n$.

7   Conclusion

In this work, we constructed and numerically implemented linearized and purely implicit finite difference analogues of the mathematical model of the collector parameters. The equation of conservation of splitting energy by physical processes: At the first stage (as a predictor), we approximated all terms of the equation with the exception of conductive heat transfer, which is numerically implemented at the second stage (as a corrector) This made it possible to determine the well bottom pressure at the first stage, i.e., a decrease in the temperature of natural gas during its flow to the surface due to the throttling effect initiated by the Joule-Thompson effect. We presented the results of the computational experiment in the form of graphs. A comparison of the calculation results for both difference schemes showed a sufficiently high accuracy of the linearized difference scheme, its solution does not differ much from the numerical solution obtained using an implicit difference scheme.

8   Acknowledgment

References

[1] L.S. Leibenzon, *Podzemnaya gidrogazodinamika*. Sobr. trudov. T.2. – Moscow: izdatelstvo AN USSR, 1953 [in Russian]

[2] B.B. Lapuk, F.A. Trebin, O sostoyanii i zadachakh dalneyshego razvitiya teoreticheskikh osnov razrabotki gazovikh mestorojdeniy – Tr. MINKH i GP.GOSINTI. 1961. [in Russian]

[3] I.A. Charny, *Podzemnaya gidrogazodinamika*. – Moscow:Gostoptechizdat, 1963. [in Russian].

[4] J. Bear, Dynamics of Fluids in Porous Media. – New York, Elsevier, 1972.

[5] S.N. Zakirov, B.B. Lapuk, *Proektirovanie i razrabotka gazovikh mestorojdeniy*. – Moscow: Nedra, 1974. [in Russian]

[6] U.P. Jeltov, *Mekhanika neftegazonosnogo plasta*. – Moscow: Nedra, 1975. [in Russian]

[7] G.I. Barenblatt, V.M. Entov, V.M. Rijik, Theory of Fluid Flows Through Natural Rocks Springer, 1990.

[8] V.I. Vasil'ev, Chislennoe integrirovanie differentsialnykh uravneniy s nelokalnymi granichnymi usloviyami. – Yakutsk: Izdatelstvo YF SO AN SSSR, 1985. [in Russian]

[9] K.S. Basniev, A.M. Vlasov, I.N. Kochina, V.M. Maksimov, *Podzemnaya gidravlika*. – Moscow: Nedra, 1986. [in Russian]

[10] A.A. Samarskii, *The theory of difference schemes*. – New York – Basel. Marcel Dekker, Inc, 2001.

[11] A.A. Samarskii, P.N. Vabishchevich, *Computational heat transfer*. – New York: Wiley. 1995.

[12] K. Aziz, A. Settari, *Petroleum Reservoir Simulation.* – Society of Petroleum Engineers, 1979.

[13] A.N. Konovalov, *Zadacha filtratsii mnogofaznoi nesjimaemoi jidkosti*. – Novosibirsk: Nauka. Sib. otdelenie. 1988. [in Russian]

[14] E.A. Bondarev, V.I. Vasil'ev, A.F. Voevodin, etc., *Termogidrodinamika sistem dobichy i transporta gaza.* – Novosibirsk: Nauka. Sib. otdelenie. 1988. [in Russian]

[15] V.I. Vasil'ev, V.V. Popov, T.S. Timofeeva, Vychislitelnie metody v rasrabotke mestorojdeniy nefti i gaza – Novosibirsk: Izdatelstvo SO RAN, 2000. [in Russian]

[16] V.V. Latonov, G.R. Gurevich, Raschet koeffitsienta sjimaemosti prirodnykh gazov // Gazovaya promyshlennost, **2** (1969), 7–9. [in Russian]

[17] K.K.Argunova, E.A. Bondarev, I.I.Rozhin, Properties of a real gas and their analytical representations// Gazohimiya, **6**:16(2010), 52-54[in Russian].

[18] M.V. Vasilyeva, V.I. Vasilyev, A.A. Krasnikov, D.Y. Nikiforov, *Numerical simulation of single-phase fluid flow in fractured porous media* // Uchenye Zapiski Kazanskogo Universiteta. Seriya Fiziko-Matematicheskie Nauki, **159**:1 (2017), 100–115. [in Russian]

[19] A.A. Afanasyev, On the Numerical Modeling of Water Flows in Porous Media under Near-Critical Conditions // Fluid Dynamics, **55**:8 (2020), 1003-1011

[20] E.A. Bondarev, A.F. Voevodin, K.K.Argunova, I.I.Rozhin, Equations of state in mathematical models of production and transportation natural gas // Siberian J. Num. Math. / Siberian Branch of Russian Academy of Science, **23**:3 (2020), 309–313. [in Russian]

[21] E. Chuvilin, G. Tipenko, B. Bukhanov, V. Istomin, D. Pissarenko, *Simulating Thermal Interaction of Gas Production Wells with Relict Gas Hydrate-Bearing Permafrost* // Geosciences. **12**:3 (2022), 115.

Vasiliy Ivanovich Vasil'ev
North-Eastern Federal University,
str. Belinsky 58,
677000, Yakutsk, Russia
Email address: vasvasil@mail.ru

Albert Vladimirovich Ammosov
North-Eastern Federal University,
str. Belinsky 58,
677000, Yakutsk, Russia
Email address: albertdobun@gmail.com